Electron-hole plasma expansion in the direct-band-gap semiconductors CdS and CdSe

F. A. Majumder, H.-E. Swoboda, K. Kempf, and C. Klingshirn
Physikalisches Institut der Universität Frankfurt, Robert-Mayer-Strasse 2-4, D-6000 Frankfurt am Main 1, Germany
(Received 26 November 1984; revised manuscript received 19 February 1985)

The properties of the electron-hole plasma in direct-band-gap semiconductors are investigated by excite- and probe-beam techniques with use of CdS and CdSe as examples. By spatially resolved transmission and reflection spectroscopy and by using samples of different thicknesses, the diffusion length and other data of the plasma are determined. A "slow drift" is found, i.e., the drift velocity is smaller than the Fermi velocities of electrons and holes. The drift distances are of the order of 10 μm with some significant differences between CdS and CdSe. Various models used in the literature to fit the observed gain spectra are critically discussed.

I. INTRODUCTION

The electron-hole plasma (EHP) has been investigated in direct-band-gap semiconductors like CdS, CdSe, or GaAs since several years by various spectroscopic techniques. Without trying to be complete, we should like to mention luminescence spectroscopy,[1-3] transmission and reflection spectroscopy by the two-beam method with fixed energy of the exciting photons $\hbar\omega_{\rm exc}$,[4-6] or with variable $\hbar\omega_{\rm exc}$ as excitation spectroscopy.[6-8] There are measurements with temporal[3,9,10] or spatial[11-13] resolution, and others under homogeneous and stationary excitation conditions.[5,12,14,15]

The results are gradually converging: an EHP is formed in all direct-band-gap semiconductors under sufficiently strong pumping. The excitation intensity $I_{\rm exc}$ necessary to produce an EHP varies from a few tens of kW/cm^2 for the III-V compound GaAs,[2,6] over some hundreds of kW/cm^2 for the II-VI compound semiconductors,[4,5,7] up to a few GW/cm^2 for the I-VII compound CuCl.[16] In the latter case, exciton and biexciton features are dominant under less extreme pumping conditions.

In direct-band-gap semiconductors with a dipole-allowed band-to-band transition, an EHP is, at low temperatures, connected with population inversion and high optical amplification (gain) of the order of 1 μm^{-1}. Small excited volumes are therefore a favorable and often necessary condition to produce and to observe an EHP.[5,15]

Early calculations based on quasiequilibrium conditions predicted a first-order phase transition to an EHP liquid for the direct-band-gap semiconductors below a critical temperature T_c, analogous to the case of the indirect-band-gap materials like Si, Ge, or GaP.[17-19] In the meantime it became clear both from experiment and theory that no liquidlike phase is formed, since the lifetime of the carriers in the plasma is so short that no clear phase separation can develop.[5,7,10,12,14,20]

On the other hand, some aspects of the EHP in direct-band-gap materials are still subject to controverse discussion. Two of them will be addressed here:

The way the gain and luminescence spectra are best fitted by a theoretical model changed with time. First, a recombination with completely relaxed **k** conservation has been favored.[4-6,21] Then **k** conservation and many particle effects have been considered.[2,22-25] Presently, some authors stress a model with **k** conservation, including an ambipolar drift of the plasma, but neglecting all many-particle effects.[19,26]

It is generally agreed that a gradient of the chemical potential of the EHP caused, e.g., by inhomogeneous excitation conditions, will lead to an ambipolar drift current. However, quite different values of the drift length l_D and the drift velocity v_D can be found in the literature: One group of authors finds from their experiments values of $v_D \lesssim 10^6$ cm/sec and $l_D \lesssim 20$ μm.[11-15] The value for v_D is below the Fermi velocities of electrons and holes, v_F^e and v_F^h, respectively. In the following this will be called "slow drift." These numbers are slightly above those calculated with the "thermo-diffusion model".[27] Some authors claim that the values of v_D are limited in polar, direct-band-gap materials even by the velocity of the acoustic phonons. The values are $10^5 \lesssim v_{\rm TA} < v_{\rm LA} \lesssim 5\times 10^5$ cm/sec.[28] In contrast, another group of authors deduce from their experiments $v_D \gtrsim 10^7$ cm/sec.[10,26,29-31] This value equals roughly the Fermi velocities of the carriers in the EHP and exceeds $v_{\rm TA,LA}$ by about 2 orders of magnitude. This case will be called "fast drift" in the following. Values of $l_D \gtrsim 100$ μm have been reported.[29-31] The main arguments come in this case from spatially resolved luminescence spectroscopy[29-31] and the analysis of gain spectra.[10,26]

It should be noted, that a similar controversy exists for indirect-band-gap materials at temperatures above T_c,[32,33] which is, however, not subject to this contribution.

The aim of this paper is to present experimental data for direct-band-gap materials which are suitable for use in the deduction of information about the state of the EHP and its expansion. CdS and CdSe have been selected as examples.

In the next section the experimental setup will be described. In Sec. III the experimental findings are presented. Section IV contains a discussion of the various possibilities, how to fit theoretical model calculations to the measured gain or luminescence spectra and the con-

clusion that may be drawn from this fit. In Sec. V follows the interpretation of the other experimental data, especially of those from spatially resolved transmission and reflection measurements.

II. EXPERIMENTAL SETUP

The experimental setup shown in Fig. 1 allows one to measure spatially and, in principle, also temporally resolved, the transmission and reflection spectra of the samples, without and with simultaneous excitation by an intense pump beam. The important features of this setup are briefly described here. For more details, the reader is referred to Refs. 14 and 15.

The central excitation source is a N_2 laser, producing pulses of about 200 kW peak power and of a temporal half-width of 10 nsec with a repetition rate of about 30 Hz, synchronized with the scan rate of the optical multichannel analyzer. The N_2 laser simultaneously pumps two dye lasers, an intense narrow-band dye laser (NDL) and a weak broadband dye laser (BDL) acting as excitation and probe sources, respectively. The spectral half-width of the NDL is $\lesssim 0.1$ meV and the pulse duration τ_{NDL} is about 5 nsec FWHM (full width at half maximum). The laser is tuned in the exciton continuum for CdS and CdSe [$\hbar\omega_{exc}(CdS)=2.587$ eV and $\hbar\omega_{exc}(CdSe)=1.847$ eV] to ensure efficient pumping of the plasma by one-photon absorption at all intensities, with a rather small excess energy in order to avoid unnecessary plasma and lattice heating. The BDL cavity is aligned to emit pulses of $\tau_{BDL}\approx 3$ nsec FWHM. The optical delay is adjusted so that the probe beam impinges on the sample at the maximum of the pump beam, resulting in almost stationary excitation conditions during the probe pulse. The dyes in the BDL are selected to emit rather flat spectra of about 50 meV total width extending from the $n=1$ $A\Gamma_5$ and $B\Gamma_5$ excitons to lower energies. Both dye-laser beams pass through pinholes (A_1 and A_2).

In one set of experiments, the diameter of A_2 is about 2–3 times that of A_1. The beams are made collinear with a partly transmitting mirror (PTM). They are polarized with $\mathbf{E}\perp\mathbf{c}$, $\mathbf{c}$ being the crystallographic axis. Finally, the two apertures A_1 and A_2 are imaged with one lens (L_2) on the sample in the cryostat. Evidently, the spot diameter of the BDL will be larger on the sample because the distances of both pinholes to the crystal are equal. This allows then to measure variations of the optical properties inside and outside the excitation spot. The temporal coincidence of the pulses and their shape is controlled during the measurement with a fast photodiode and an oscilloscope and their spatial coincidence by a microscope, not shown in Fig. 1. The maximum intensity of the NDL on the sample is about 5 and 2 MW/cm^2 in the cases of CdS and CdSe, respectively, limited by the damage threshold. It can be decreased by neutral-density filters. The intensity of the BDL is kept at values where all variations of the optical properties induced by the BDL can be excluded. The transmitted or reflected BDL beam and the sample are then magnified in a plain by L_3 or L_4, respectively. The factor of magnification is selected to be 10 (5) for CdS (CdSe). In this plane the end of a multimode fiber optics can be moved in both axes perpendicular to the beam with a micrometer screw. The core diameter of the fiber optics is 50 μm. This allows scanning over the excitation spot, with a spatial resolution of 5 μm (10 μm) on the crystal. The output of the fiber optics is imaged on the entrance slit of a 1-m spectrometer. The wavelength-dispersed spectrum is detected by a SIT vidicon tube and subsequently digitalized, stored, and handled in an OMA-II system. Figure 2 shows the spatial profiles of the pump and the probe beams on the sample measured with the setup described above for the case of CdS. This type of measurement evidently yields information about the lateral drift or expansion of the EHP.

In a second set of experiments we have chosen the diameter of A_2 to be about one-third that of A_1. Consequently, the excited sample is probed in this case temporally and spatially in the center of the excitation spot. The probe beam is sent once on the excited surface of the sample and once on the opposite one. In both cases the transmitted and reflected probe beams are analyzed with respect to plasma gain and excitonic reflection. By using samples of various thicknesses d ($2.0\lesssim d\lesssim 40$ μm), this type of experiment gives information about the longitudinal drift, i.e., the expansion of the plasma into the depth of the sample.

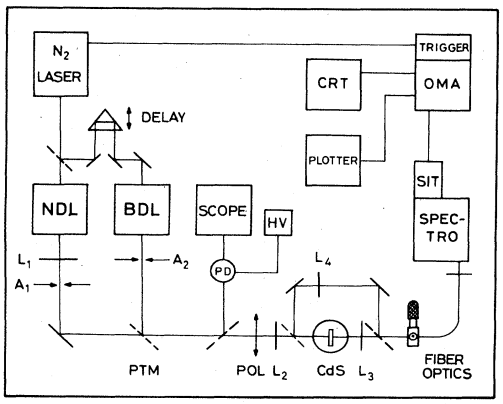

FIG. 1. A setup which allows one to measure, spatially resolved, the transmission and reflection spectra of a sample with the excite-and-probe technique.

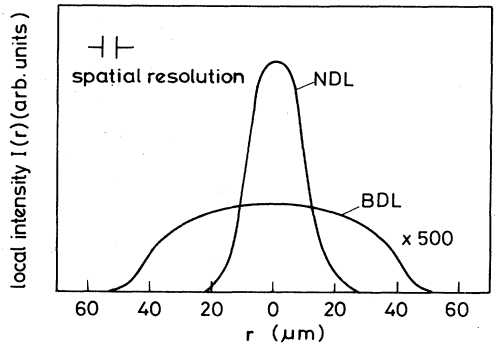

FIG. 2. Lateral spatial profiles of the two dye-laser beams NDL and BDL on the sample, measured with the setup sketched in Fig. 1. r is the distance from the center of the excitation spot.

The samples used are high-quality platelets, with the c axis in the platelet plain. The thicknesses of the samples range between 2 and 38 μm in the case of CdS and between 5 and 20 μm for CdSe. The thinner ones are excited homogeneously in depth. Samples are selected that show sharp excitonic reflection structures. Unfortunately, it turned out that the CdSe samples are damaged in the center of the excitation spot after a few pulses under conditions where an EHP is formed. Therefore no reflection spectra have been taken for this material and the transmission spectra from the damaged region are suppressed. The samples are mounted strain free in a He-evaporation cryostat, which allows variation of the lattice temperature T_L from 5 K to higher values.

The main information deduced from the experiments described in the following comes from the analysis of the spectra of optical amplification, (gain) $g(\hbar\omega)$, connected with an EHP at low temperatures in the semiconductors under consideration, and from the dependence of the absolute value of amplification and of excitonic reflection as a function of the sample thickness.

III. EXPERIMENTAL RESULTS

In the first subsection, data for CdS are reported, and in the second, for CdSe.

A. CdS

The data obtained with the setup described above at the center of the excitation spot for samples with a thickness $d \lesssim 3$ μm can be considered as characteristic for a stationary, nondrifting plasma. There are almost no temporal variations of $I_{\text{exc}}(t)$ and the plasma density n_p during the probe pulse since we have $\tau_{\text{NDL}} > \tau_{\text{BDL}} \gg \tau_p$, τ_p being the lifetime of the electron-hole pairs in the plasma (see Sec. V). There are no lateral gradients in the center of the spot, and samples of this thickness are almost homogeneously excited in the depth because the diffusion length l_D is of the order of d. The last point can also be considered from another point of view: The absorption coefficient at $\hbar\omega_{\text{exc}}$ is around 10^5 cm^{-1}. The penetration depth of the pump laser is thus about 0.1 μm. If l_D is significantly below 1 μm, the sample is nonhomogeneously excited in depth, but in this case v_D is so low ($v_D \lesssim 5\times 10^5$ cm/s) that the influence of v_D on the spectra of the EHP can be completely neglected. If, on the other hand, $l_D \gtrsim 3$ μm, the longitudinal drift is suppressed by the one-dimensional confinement of the EHP. A fast longitudinal drift should show up in a significant variation of the gain spectra in thicker samples without confinement. Figure 3 shows a set of gain spectra $g(\hbar\omega)$ for various values of the excitation intensity I_{exc}, deduced from the transmission spectra of the unexcited and the excited sample, I_T and I_T^*, respectively, according to Refs. 5 and 7. If necessary, the luminescence has been subtracted from I_T^*. The modulation of $g(\hbar\omega)$, caused by the shift of the Fabry-Perot modes of the platelet-type samples, with increasing excitation,[7,8] has been averaged out in such a way that the smooth curve passes through the modulation structures at half-height, thus keeping the value of G (see below) constant. As in the case without spatial resolution,[7] one finds that the energy $\hbar\omega_{\text{co}}$ of the crossover between gain and absorption shifts to the red with increasing I_{exc}. Furthermore, the spectral width of the gain spectra and the integral gain G increase with I_{exc}. G is defined as

$$G = \int_0^{\hbar\omega_{\text{co}}} g(\hbar\omega)\, d(\hbar\omega) \,. \tag{1}$$

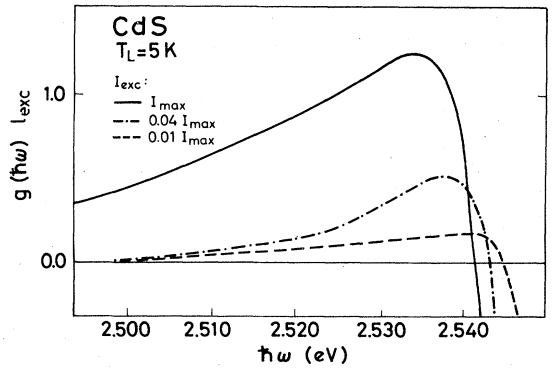

FIG. 3. Gain spectra $g(\hbar\omega)$ of the EHP in CdS under stationary and homogeneous excitation conditions measured for three different excitation conditions. The excitation depth l_{exc} is given by the diffusion length l_D or the sample thickness d, whichever is shorter.

Figures 4 and 5 contain some addition information with which to supplement Ref. 7. Figure 4 shows the red shift of the chemical potential with increasing lattice temperature at I_{exc}=const=4 MW/cm^2. Figure 5 shows the red shift of $\hbar\omega_{\text{co}}$ with increasing I_{exc} with the lattice temperature as a parameter. When $T_L < 50$ K (open symbols) the red shift is less pronounced than for higher temperatures (solid symbols).

There is not a systematic variation of the shape of $g(\hbar\omega)$ with the sample thickness. Gain appears both in the transmitted and reflected probe beam.[4,14,16]

In Fig. 6(a) we give the maximum of $\ln(I_T^*/I_T)$ for transmission experiments as a function of the sample thickness. This quantity equals rather precisely the product of gain times the depth of the excited volume $g_{\max} l_{\text{exc}}$,

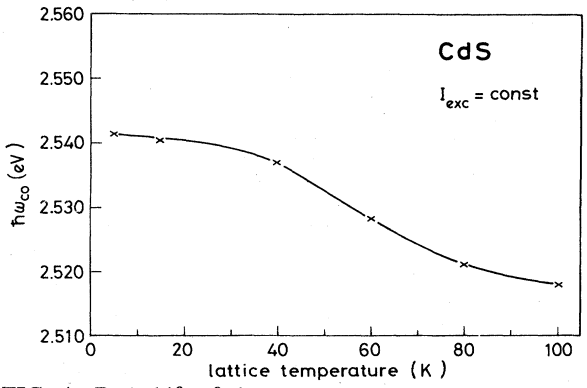

FIG. 4. Red shift of the crossover energy $\hbar\omega_{\text{co}}$ of the EHP gain spectra in CdS with increasing lattice temperature T_L, at constant excitation conditions (I_{exc}=4 MW/cm^2, $\hbar\omega_{\text{exc}}$=2.587 eV).

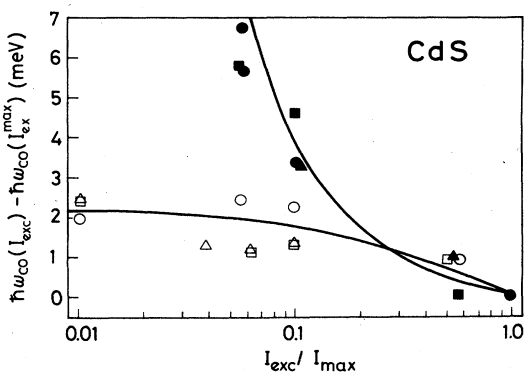

FIG. 5. Shift of the crossover $\hbar\omega_{co}$ as a function of the excitation intensity, measured relative to its position at maximum excitation $I_{exc}^{max}=5$ MW/cm^2 ($\hbar\omega_{exc}=2.587$ eV). Parameter is the lattice temperature: $T_L=5$ K (△), 15 K (○), 40 K (□), 60 K (△), 80 K (■), and 100 K (●). The solid lines only guide the eye in the two temperature regions $T_L \gtrless 50$ K.

since the unexcited sample is transparent around 2.53 eV and since the index of refraction changes only slightly in this spectral region.[8,34] The straight solid and dashed lines are averages over the experimental points for two different excitation intensities and shall guide the eye. The curve necessarily starts from the origin. It increases with sample thickness, but saturates for $d \gtrsim 4$ μm. The experimental values fluctuate around 0.5 and 0.8, respectively, for the two different excitation intensities. These fluctuations show the "quality" of the individual sample and make it rather hazardous to draw conclusions from only two samples, as is done for CdTe.[19]

It is well known that the excitonic reflection structures disappear if an EHP is created (see, e.g., Refs. 5, 12, and 35). In Fig. 6(b) we give as a function of d the variation

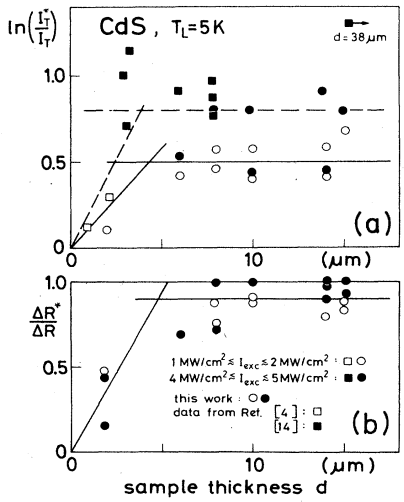

FIG. 6. (a) Maximum values of the quantity $\ln(I_T^*/I_T)$ as a function of the sample thickness d, measured in transmission for two different values of the excitation intensity I_{exc}. (b) Normalized variation of the excitonic reflection $\Delta R^*/\Delta R$ measured on the unexcited surface of the sample as a function of d for two different values of I_{exc}.

ΔR^* between the reflection maximum and minimum for the $A\Gamma_5$ ($n=1$) exciton resonance, measured at the center of the excitation spot, but on the nonexcited surface of the sample, and normalized by the value ΔR of the unexcited sample. Since the excitonic structures disappear completely in the center of the excitation spot on the excited surface (Ref. 12 or Fig. 7), i.e., for $d=0$, the curve must again start from the origin. With increasing d, $\Delta R^*/\Delta R$ grows and recovers the value of the unexcited sample above $d \approx 5$ μm. A small additional damping of the exciton leading to $\Delta R^*/\Delta R = 0.9 \pm 0.1$ can be caused simply by irradiation of the unexcited sample surface with the probe beam or the luminescence of the sample. Almost identical data are found for the $B\Gamma_5$ ($n=1$) resonance.

Figures 7 and 8 make use of the lateral spatial resolution of the setup. Figure 7 gives the following quantities as a function of the distance r from the center of the excitation spot: the profile of the excitation beam $I_{exc}(r)$ (△), the integrated gain $G(r)$ (□), and the modulation of the excitonic reflectivity $\Delta R^*(r)=R_{max}-R_{min}$ of the $A\Gamma_5$ ($n=1$) exciton (○) measured now on the excited surface of the sample. One sees that the profile of $G(r)$ directly reproduces $I_{exc}(r)$. $\Delta R^*(r)$ is zero at the center of the excitation spot, but recovers the value of the unexcited sample (→) just outside the excitation spot. The features described above are independent of the excitation intensity when in the MW/cm^2 range. They do not change for variations of the excitation-spot diameter from 10 to 50 μm and of the lattice temperature from 5 to 120 K.

To obtain additional information about a possible drift of the EHP, we measured the gain spectra at the same local excitation intensity, $I_{exc}(r)=1.5$ MW/cm^2, once in the center of the excitation spot and once on its flank, as shown in the inset of Fig. 8. The two gain spectra almost coincide, with the exception of a slight red shift of $\hbar\omega_{co}$ at the flank. The slope around $\hbar\omega_{co}$ decreases only slightly when going from the center to the flank.

B. CdSe

The data of Figs. 9—12 are measured, for CdSe, close to the center of the excitation spot, but outside the damaged

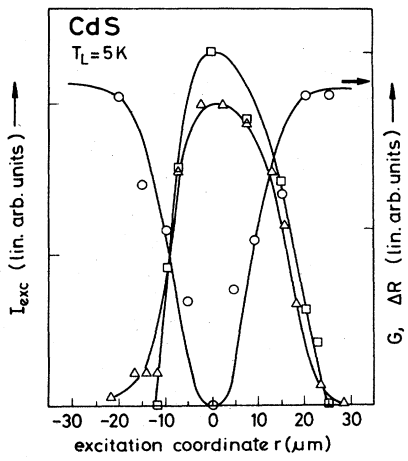

FIG. 7. Spatial profile of the excitation spot (△), the integral gain G (□), and the modulation ΔR of the reflectivity at the $n=1$ $A\Gamma_5$ resonance (○).

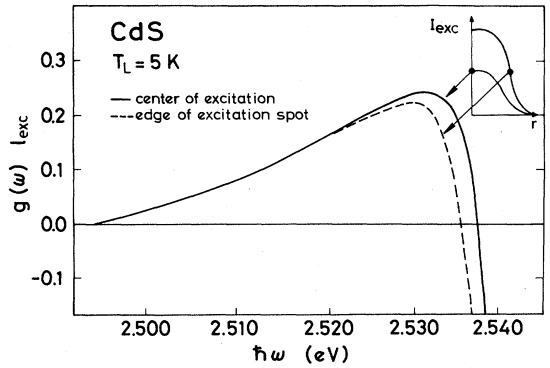

FIG. 8. Two gain spectra taken under identical local excitation intensities I_{exc}^{loc} at the center of the excitation spot and on its flank, as indicated in the inset ($I_{exc}^{loc}=1.5$ MW/cm^2, $\hbar\omega_{exc}=2.587$ eV).

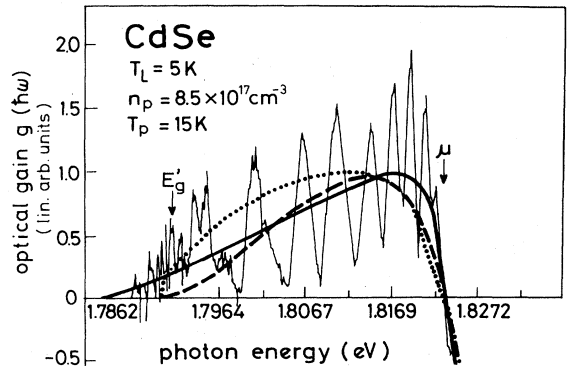

FIG. 10. Gain spectrum resulting from Fig. 9, together with three curves calculated for $v_D=0$, $n_p=8.5\times10^{17}$ cm^{-3}, and $T_p=15$ K. Dotted line, model with **k** conservation; dashed line, model without **k** conservation; solid line, model with **k** conservation, energy-dependent damping, and excitonic enhancement.

area. Figure 9 shows I_T and I_T^* for a 5-μm-thick sample. The increase of absorption above $\hbar\omega_{co}$ and the optical amplification below it are obvious. The spectra are modulated by the Fabry-Perot modes (FP) of the platelet-type sample. There is also a blue shift of the modes with increasing excitation, as in the case of CdS.[7,8,34]

Figure 10 gives the gain spectrum deduced from I_T and I_T^*. The modulation is due to the shift of the modes. The smooth solid, dashed and dotted lines are curves calculated with different models and $v_D=0$. They will be discussed in Secs. IV and V. The solid line coincides almost perfectly with the experimental one, if the modulations due to the shifting FP modes are averaged out in the way described above.

Figure 11 shows gain spectra for various values of I_{exc}. As in CdS, the height and width of the spectra increase with I_{exc}. However, in contrast to CdS, $\hbar\omega_{co}$ now shows a slight blue shift with increasing I_{exc}.

Figure 12 gives the integrated gain G as a function of I_{exc}. G increases first linearly with I_{exc} and then tends to saturate above 1.5 MW/cm^2. This behavior is similar to that of CdS.[7] Figure 13 corresponds to Fig. 4 for CdS and shows the temperature dependence of $\hbar\omega_{co}$ for constant I_{exc}. The function decreases in both cases monotonically in the investigated range of temperatures. Figure 14 finally shows gain spectra for three samples of various thicknesses ranging from $5\leq d\leq 9$ μm. The peak values of $g(\hbar\omega)$ and G increase sublinearly with d. An increase of d by a factor of 2 results in an increase of $\ln(I^*/I)=g_{max}l_{exc}$ of only 25%.

Figures 15 and 16 again make use of the spatial resolution of the setup. Figure 15 gives the normalized integrated gain G as a function of the distance r from the center of the excitation spot. The radius of the excitation spot is about 20 μm. In contrast to CdS, gain is observed in this case outside the excitation spot. G decays to one-half of its maximum value over a distance of about 20 μm outside the excitation spot. With increasing distance from the center of the excitation spot, the width of the gain spectrum decreases, indicating a decrease of n_p. In connection with Fig. 11, this explains the red shift of $\hbar\omega_{co}$ with increasing r, as shown in Fig. 16.

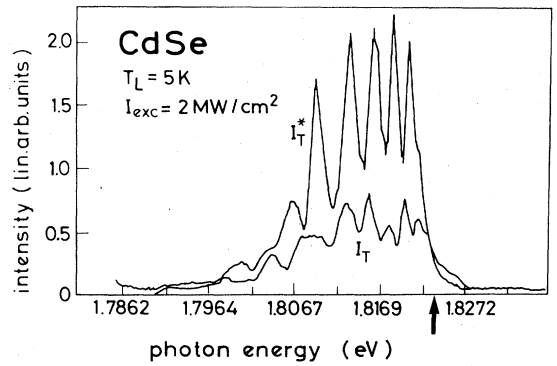

FIG. 9. Transmission spectra of the BDL through a 5-μm-thick CdSe platelet without and with additional excitation, I_T and I_T^*, respectively. The arrow indicates $\hbar\omega_{co}$.

IV. HOW TO FIT THE GAIN SPECTRA

The information that may be deduced from the gain spectra depends significantly on the model used to fit them: Concerning the direct-band-gap materials, there was a certain evolution concerning the question of what is considered to be "state of the art." Assuming that all excitonic correlations are screened in an EHP, one would expect, in a direct-band-gap material in the simplest case

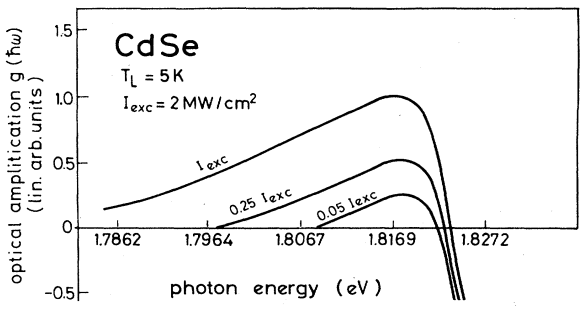

FIG. 11. Gain spectra of CdSe under stationary and homogeneous excitation conditions for various excitation intensities.

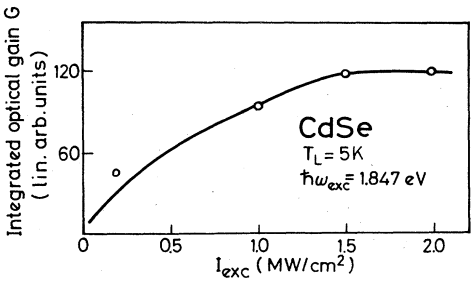

FIG. 12. Integrated optical gain as a function of the excitation intensity I_{exc} for CdSe.

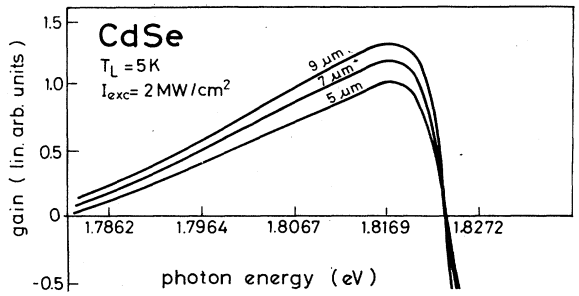

FIG. 14. Gain spectra of CdSe for constant excitation conditions and various sample thicknesses d.

(parabolic bands), gain and luminescence spectra, $g(\hbar\omega)$ and $l(\hbar\omega)$, respectively, given by the square-root dependence of the combined density of states above the reduced gap $E_g'(n_p)$ and modulated by the Fermi functions of electrons and holes, f_e and f_h:

$$g(\hbar\omega)\sim[\hbar\omega-E_g'(n_p)]^{1/2}(f_e+f_h-1)\ ,\quad \hbar\omega>E_g'$$
$$l(\hbar\omega)\sim[\hbar\omega-E_g'(n_p)]^{1/2}(f_e+f_h)\ ,\quad \hbar\omega>E_g' \qquad (2)$$
$$g(\hbar\omega)=l(\hbar\omega)=0\ ,\quad \hbar\omega<E_g'\ .$$

Examples of $g(\hbar\omega)$ calculated according to (2) are given in Figs. 10 and 20. This square-root increase of $g(\hbar\omega)$ or $l(\hbar\omega)$ at the low-energy edge has never been observed in any experiment (e.g., Refs. 1–16). The spectra always start slightly superlinearly at their low-energy edges, i.e.,

$$g(\hbar\omega),l(\hbar\omega)\sim(\hbar\omega-E_g')^{\alpha}\ \text{for}\ \hbar\omega\gtrsim E_g'\ , \qquad (3)$$

with $1<\alpha<2$. With such behavior being known from the indirect-band-gap materials, where the **k** conservation is relaxed by the participation of a phonon, one used a heuristic "no-**k**-conservation model" to fit the gain spectra.[5–7,21] This model gave reasonable agreement between experiment and theory (see, e.g., Ref. 7 or Fig. 10), although it lacks the justification from first principles.

The situation improved considerably when a model was developed that started with **k** conservation and included many-particle (MP) effects. See, e.g., Refs. 22 and 23, and 24 and 25 for recent reviews. Two of these effects are of special importance. One is a **k**-dependent damping of the electron and hole states evoked by the recombination of an electron-hole pair. This damping is smallest around the Fermi vector $\mathbf{k}_F$ and increases roughly quadratically with $|\mathbf{k}-\mathbf{k}_F|$.[24] It has the consequence that $l(\hbar\omega)$ and $g(\hbar\omega)$ are smeared out around E_g', transforming the square-root behavior into the experimentally found behavior. The gain and luminescence spectra then extend to values somewhat below E_g' (Fig. 10). The other term is the so-called excitonic enhancement. It describes a part of the electron-hole pair correlation still present in the plasma. This correlation and the related increase of the oscillator strenght are strongest around the chemical potential μ of the electron-hole pairs in the plasma, because, there, occupied and empty states coexist.[22–25] Figure 17 gives some examples for CdS. The behavior for CdSe is qualitatively the same.[15] The influence of the excitonic enhancement is mainly to increase the slope of the transition from gain to absorption in $g(\hbar\omega)$ (Fig. 10 and Ref. 7), and to shift the maxima of $l(\hbar\omega)$ and $g(\hbar\omega)$ somewhat toward higher energies. The spectra calculated with this model are in quantitative agreement with experimental data. See Fig. 10 or Refs. 2, 7, and 13–15.

Recently, it has been argued that the EHP might be subject to a drift under inhomogeneous excitation conditions,[11,19,26] the electrons and holes having the same drift velocity v_D for reasons of neutrality.[12] The drift of the carriers can be described by modified Fermi functions,

$$f_{e,h}=\left[\exp\left[\frac{\hbar^2}{2m_{e,h}k_BT_p}(\mathbf{k}\pm\mathbf{k}_{D_{e,h}})^2-\frac{E_{F_{e,h}}}{k_BT_p}\right]+1\right]^{-1}, \qquad (4)$$

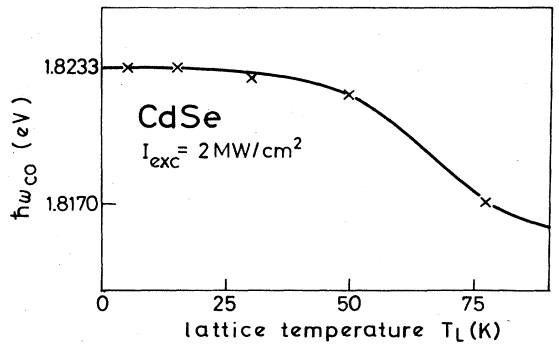

FIG. 13. Energy $\hbar\omega_{co}$ of the crossover from gain to absorption as a function of the lattice temperature T_L under constant excitation.

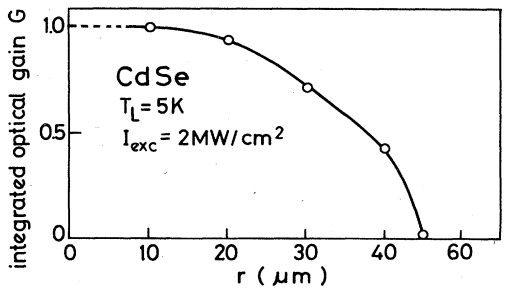

FIG. 15. Integrated optical gain G as a function of the distance r from the center of the excitation spot. The radius of the excitation spot is about 20 μm.

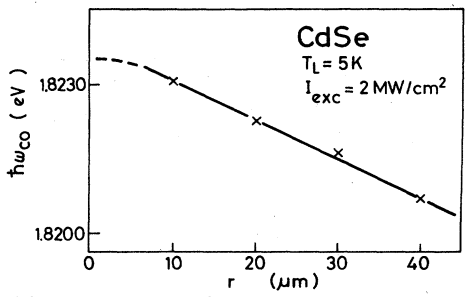

FIG. 16. Dependence of $\hbar\omega_{co}$ on the distance r from the center of the excitation spot.

with $\mathbf{k}_{D_{e,h}}=(m_{e,h}/\hbar)\mathbf{v}_D$. For parabolic bands the quasi-Fermi-levels $E_{F_{e,h}}$, and the chemical potential $\mu=E_{F_e}-E_{F_h}$, are independent of v_D for given values of n_p and T_p. The influence of k_D becomes important when the kinetic energy $E_D=\hbar^2k_{D_{e,h}}/2m_{e,h}$ related to the drift vector k_D becomes comparable to the one related to the Fermi vector. Figure 18 gives calculated Fermi functions for various values of v_D for CdS. Plotted as a function of energy, the modified Fermi functions become flatter with increasing v_D. The value $f=\frac{1}{2}$ shifts to lower energies due to the square-root dependence of the density of states. Again, the curves for CdSe are almost identical.[15] If $\mathbf{k}$ conservation is used, the value of $\hbar\omega_{co}$ shifts from μ to lower energies. Figure 19 gives the calculated shift for CdS and CdSe.

Recently, a model has been stressed to fit the gain spectra of a drifting plasma which takes into consideration only recombination under $\mathbf{k}$ conservation [Eq. (2)] and the Fermi function of Eq. (4), neglecting all other contributions such as damping or excitonic enhancement.[19,26] Figure 20 shows a set of spectra calculated for CdS with this model. It is clear from Eqs. (2) and (4) that the gain spectrum will always start with infinite slope at E_g'. However, for drift velocities $v_D \gtrsim v_{F,h}$, gain spectra are produced that roughly start as described in Eq. (3).

As can be seen from Fig. 10 and from Fig. 22 below, it is possible to fit an experimentally observed gain spectrum

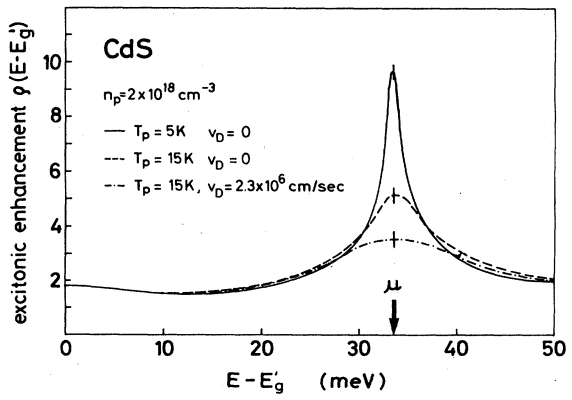

FIG. 17. Excitonic enhancement ρ as a function of the energetic distance from the reduced gap E_g' for constant plasma density n_p and various values of the plasma temperature T_p and drift velocity v_D.

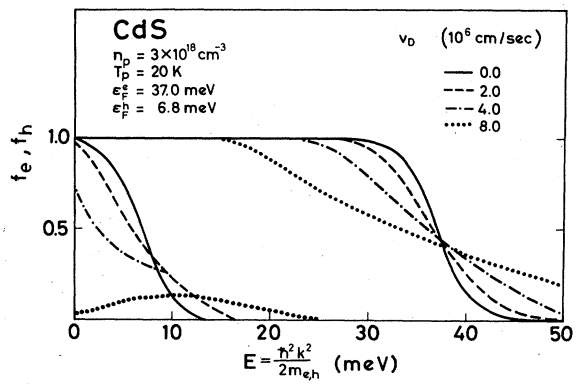

FIG. 18. Calculated Fermi functions f_e and f_h for electrons and holes for various values of the ambipolar drift velocity v_D for CdS as a function of the kinetic energy of the carriers, E.

either by taking into account many-particle effects or nonequilibrium (NE) effects, i.e., drift. The plasma parameters deduced in both cases are significantly different, however. A fit to a gain spectrum of a given, experimentally determined width gives an increasing value of n_p with increasing v_D, with all other parameters unchanged. Therefore, arguments must be found to decide under which experimental condition MP or NE effects are predominant.

A first conclusion can be drawn from measurements in which the EHP is subject to three-dimensional confinement. Such experiments have been reported for $Ga_{1-x}Al_xAs_x$ in Ref. 2. NE effects are excluded under these conditions. The luminescence spectra can only be fitted by using MP effects in the way described above. The same conclusion can be drawn from the gain spectra of CdS taken at the center of the excitation spot for thin samples ($d \leq 3$ μm). As mentioned in Sec. III A, lateral drift is suppressed by symmetry arguments, while longitudinal drift is either negligible ($l_D < d$) or quenched by one-dimensional confinement ($l_D \geq d$). Again, a good fit is reached only by including MP effects in the calculation, e.g., Refs. 4 and 14.

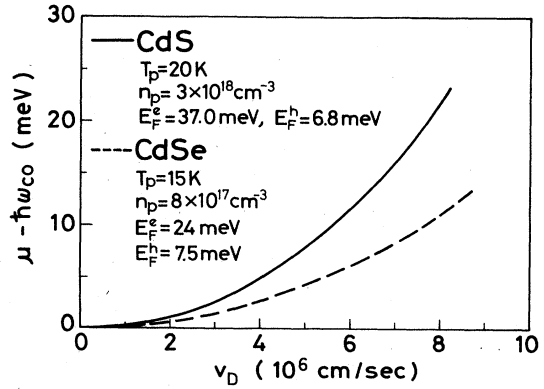

FIG. 19. Shift of the crossover $\hbar\omega_{co}$ with respect to the chemical potential μ as a function of the ambipolar drift velocity v_D for CdS and CdSe. The parameters are given in the figure. The Fermi velocities deduced from the Fermi energies are, for CdS, $v_F^e=2.5\times10^7$ cm/sec and $v_F^h=0.5\times10^7$ cm/sec; and, for CdSe, $v_F^e=2.4\times10^7$ cm/sec and $v_F^h=0.7\times10^7$ cm/sec.

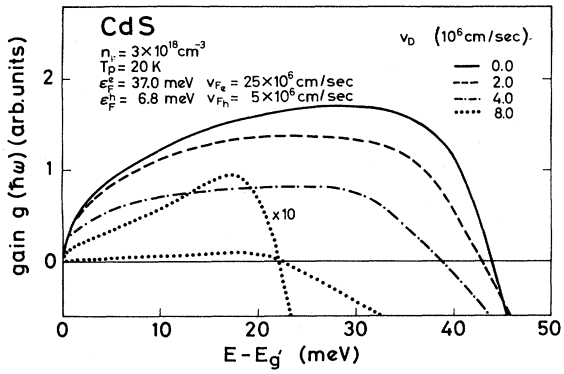

FIG. 20. Calculated gain spectra for CdS using only **k** conservation and drift.

Consequently, we can state that MP effects must always be taken into account when calculating the optical properties of an EHP. If an EHP has the possibility of expanding, NE effects must also be considered, but not exclusively.

The influence of NE effects on the Fermi functions and the excitonic enhancement can be seen from Figs. 17 and 18. It results in a red shift of $\hbar\omega_{co}$ and a considerable decrease of the slope around $\hbar\omega_{co}$, as shown in Fig. 21, where two gain spectra have been calculated for $v_D=0$ and 2.3×10^6 cm/sec, with all other parameters unchanged. The low-energy tail of the spectrum is not altered. The calculated curves of Fig. 21 can be compared to the measured ones of Fig. 8 since the scales for two curves are identical within one figure. For the curve measured in the center, significant drift can be excluded by the arguments given above. The experimentally observed red shift of $\hbar\omega_{co}$ observed on the flank leads, with Fig. 19, to $v_D=2.3\times10^6$ cm/sec, if attributed to drift alone. As seen from Fig. 21, this considerably reduces the slope around $\hbar\omega_{co}$, in contrast to the experiment. Thus it can be concluded that, for the lateral drift velocity holds, $0<v_d<2.3\times10^6$ cm/sec. These values of v_D have only a minor influence on the line shape. The shift of $\hbar\omega_{co}$ can only partly be attributed to drift; it is also partly due to other effects, such as small local variations of n_p and/or T_p.

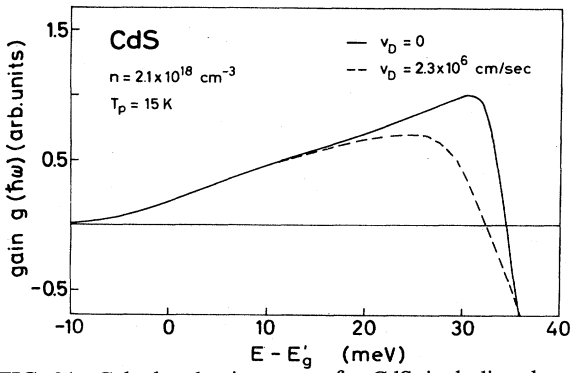

FIG. 21. Calculated gain spectra for CdS, including damping and excitonic enhancement for $v_D=0$ and 2.3×10^6 cm/sec.

The experimental finding that the EHP gain spectra do not change significantly with increasing d, i.e., under conditions where there is no more confinement, demonstrates that the longitudinal drift velocity is also so small that it has no appreciable influence on the line shape. Thus we can conclude from the line-shape analysis that under the experimental conditions outlined in Sec. II both the lateral and longitudinal drift velocities are smaller than the Fermi velocities of electrons and holes, and that here they have only a marginal influence on the EHP gain spectra.

After considering the line shape, some thoughts should be devoted to the spectral position of $E_g'(n_p)$ relative to the free exciton energy of the unexcited sample. The calculation of this quantity is, in polar materials, far from being trivial. The calculation must start from the bare band gap. In the case of the exciton, the reduction of the gap due to polaron corrections and the Coulomb interaction must be subtracted, where the first quantity is partly quenched for the exciton ground state if the exciton Bohr radius and the polaron radius are comparable. This is the case in CdS.[36,37] For the EHP, exchange-correlation effects must be included, as well as a dielectric function governed by the plasmon-phonon mixed states.[25,34,36] As a consequence, two rather large quantities must be compared [in CdS around 150 meV (Refs. 36 and 37)], and only their difference gives the energetic distance between the exciton at low densities and $E_g'(n_p)$. Often, calculations are applicable only for either the low- or high-density regime. Usual high-density approximations tend to converge, for $n_p\rightarrow0$, to the polaron gap and not to the free-exciton state, as they should. Theories which describe the optical properties over the entire density range from the exciton to the EHP including the delicate intermediate densities, are found in Ref. 25. They coincide with experiment without considering NE effects. Despite the difficulties outlined briefly above, the analysis of the EHP data in $Ga_{1-x}Al_xAs$ with respect to $E_g'(n_p)$ under three-dimensional confinement gave excellent agreement between experiment and theory using MP effects without drift.[2] For CdS it has already been shown in Ref. 7 that the curves deduced from the experimental gain spectra for $E_g'(n_p)$ and $\mu(n_p,T_p)$ using MP effects without drift are in good agreement with theory.[22] For CdSe there is also reasonable agreement between calculated values of $E_g'(n_p)$ and those deduced from the line-shape fit using MP effects but no drift.[15]

V. EVALUATION OF THE EXPERIMENTAL RESULTS AND DISCUSSION

First, we discuss the results obtained in the center of the excitation spot, where drift phenomena can be excluded. The data of Figs. 3 and 11 prove once again that the plasma does not reach its liquidlike equilibrium state. The width of the gain spectra, and thus n_p, increases significantly with I_{exc}, in contrast to what is expected for a liquidlike state. The variation of $\hbar\omega_{co}$ with I_{exc} is less pronounced. $\hbar\omega_{co}$ can be identified with μ for $v_D<v_F^{e,h}$. As discussed above, this is fulfilled in the center of the excitation spot, i.e., in Figs. 3 and 11.

The weak variation of μ with I_{exc} is in agreement with

theory,[7,36,37] which shows that the curves $\mu(T_p,n_p)$ are rather flat over a broad range of n_p values below the equilibrium density.[36,37] In the past, this behavior of μ has been used erroneously several times as a sufficient argument to claim the existence of a liquidlike plasma phase, e.g., in CdS or CdSe.

The decrease of $\hbar\omega_{co}$ with increasing T_L (Figs. 4 and 13) reproduces mainly the temperature dependence of the Fermi functions and the band gap.

The calculated curves in Fig. 10 show that in CdSe the best fit is obtained with the model taking into account **k** conservation, damping, and excitonic enhancement. The calculated curve coincides almost perfectly with a curve where the modulation due to the shift of the Fabry-Perot modes is averaged out (see Sec. III). The same result has been also found for CdS or GaAs.[2,7,13,14,23–25]

The sublinear increase of G with I_{exc} (Fig. 12 and Ref. 7) can be explained qualitatively by a decrease of the effective carrier lifetime τ_p with increasing n_p, caused by stimulated emission and the quadratic recombination mechanism.

Figures 3 and 5 show that the crossover $\hbar\omega_{co}$, and thus μ, decreases with increasing I_{exc} in CdS at low temperatures. This means that $\partial\mu/\partial n_p$ is negative. A region in which this condition is fulfilled exists for $T_p < T_c$ below the equilibrium density of the plasma.[36,37] Indeed, the experimental values of n_p are below the calculated equilibrium values in CdS in $n_0 = 5\times10^{18}$ cm^{-3}.[36] The phase separation that would occur in an equilibrium state under these conditions is suppressed by the short lifetime τ_p.[7,20] The stronger variation of $\hbar\omega_{co}$ with I_{exc} in CdS above 60 K may be attributed to the superposition of various recombination processes, as already discussed in Ref. 7.

In contrast to CdS, CdSe here shows a different behavior with $\partial\mu/\partial n_p > 0$. In CdSe, the calculated values of n_0 are about $(5–8)\times10^{17}$ cm^3.[36,37] This means that the experimentally observed values of n_p are around or even larger than n_0. Indeed, one has $d\mu/dn_p > 0$ in this regime.[36,37]

In the following we concentrate on the question of the drift length l_D and the drift velocity v_D under inhomogeneous excitation conditions. By l_D we mean the distance the carriers in the EHP move away from the place where they have been excited during their lifetime under the influence of the inhomogeneous excitation outlined in Sec. II. The lifetime of the carriers in the plasma, τ_p, is then connected with l_D and v_D by

$$l_D = v_D\tau_p \ . \tag{5}$$

The data shown in Fig. 7 give an upper limit for the lateral drift length by the spatial resolution of the setup, i.e., $l_D \lesssim 5\ \mu$m.

Values of this order of magnitude may be concluded from other experiments also. Efficient laser-induced gratings have been observed in CdS due to the formation of an EHP—by Saito[10] and by us.[38,39] The efficiency of the grating tends to zero, if the lateral drift length of the carriers becomes comparable to the lattice constant of the grating Λ. In Refs. 38 and 39, nsec excitation pulses have been used and the lattice spating Λ was about 17 μm. From this, it follows that $l_D < \Lambda \approx 17\ \mu$m. In psec, temporally resolved experiments,[10] values of $2.4 \lesssim \Lambda \lesssim 9.6\ \mu$m have been used. From these data it can be seen that the maximum grating efficiency decreases with decreasing Λ, the decrease being, however, more pronounced for $\Lambda < 4.6$ μm than above it. This indicates, also, values of l_D around 4 μm.

The longitudinal drift into the depth of the excited sample is also around 4 μm. This follows from the fact that the product $g(\hbar\omega)\times l_{exc}$ starts to become independent of the sample thickness d for $d \lesssim 4\ \mu$m, while $g(\hbar\omega)\times l_{exc}$ decreases for values of $d \lesssim 3\ \mu$m [Fig. 6(a)].

The same conclusion can be drawn from the data of Fig. 6(b), where the excitonic reflection is measured on the unexcited surface of the sample. For d around 5 μm the reflection structures of the A and B excitons have almost fully recovered, indicating that the EHP does not reach the opposite side of the sample, in contrast to $d < 5\ \mu$m. A similar result has also been found in Ref. 35 by measuring the excitonic reflectivity of CdS platelets 0.5—5 μm thick at the excited and unexcited surfaces. In order to find the same decrease of the excitonic reflection structure at the unexcited surface as compared to the excited one, I_{exc} had to be increased by a factor of 4, indicating a value of l_D comparable with the sample thickness.

As a conclusion of the discussion of the data for CdS, it can be stated that the longitudinal drift length under inhomogeneous excitation conditions (absorption length of the light $< 1\ \mu$m and only a few meV of excess energy) is about 4 μm. An upper value of the lateral drift distance is 5 μm. Since the lateral gradient of the generation rate is, in our experiments, almost comparable to the longitudinal one, it seems not unreasonable to assume that the longitudinal and lateral drift lengths are roughly equal.

In Sec. IV we found an upper limit for $v_D \approx 2.3\times10^6$ cm/sec. The upper limits of l_D and v_D being known, a value of τ_p may be found from Eq. (5). With $l_D \lesssim 4\ \mu$m and $v_D \lesssim 2\times10^6$ cm/sec, we obtain $\tau_p \approx 200$ psec. This value is in good agreement with the data in Refs. 10 and 40. Another crosscheck of the parameters can be deduced from the relation between the generation rate G^*, I_{exc}, and the other plasma parameters. We have

$$n_p = G^*\tau_p \ , \tag{6a}$$

$$G^* = \frac{I_{exc}}{\hbar\omega_{exc} l_D} \ , \tag{6b}$$

and, with (5),

$$n_p = G^*\tau_p = \frac{I_{exc}\tau_p}{\hbar\omega_{exc} l_D} = \frac{I_{exc}}{\hbar\omega_{exc} v_D} \ . \tag{7}$$

Equation (6b) holds because the penetration depth, $\alpha^{-1}(\hbar\omega_{exc})$, of the exciting light, l_D, and d fulfill, in our experiments, the relation

$$\alpha^{-1}(\hbar\omega_{exc}) \ll l_D \lesssim d \ . \tag{8}$$

With $v_D = 2\times10^6$ cm/sec and $I_{exc} = 2$ MW/cm^2, we obtain, from Eq. (7), $n_p = 2.5\times10^{18}$ cm^3. This value is in good agreement with the experimental data. As a consequence, the set of data given for CdS in Table I can be considered to be consistent. Larger deviations (e.g., as-

TABLE I. Plasma parameters for CdS and CdSe at a lattice temperature around 5 K.

	CdS	CdSe	Comment
	Parameters used in the fit[a] (from [28,43])		
Electron mass m_e	$0.205 m_0$	$0.13 m_0$	
Hole mass $\overline{m}_h$	$1.1 m_0$	$0.59 m_0$	$\overline{m}_h=(m_{h\perp}^2 m_{h\parallel})^{1/3}$
Exciton energy E_{ex} (eV)	2.5521	1.8252	$A\Gamma_6$
Exciton binding energy E_{ex}^b (meV)	28	17.5	
Bohr radius a_{ex} (nm)	2.8	4.72	
Dielectric constant	8.6	9	
Excitation intensity I_{exc} (MW/cm^2)	1—4	0.5—2	In CdSe lower than measured value because of surface damage
	Parameters deduced from the fit		
Plasma density n_p (cm^{-3})	$(1—4)\times10^{18}$	$(5—9)\times10^{17}$	Increasing with I_{exc}
Carrier lifetime τ_p (psec)	200±50	400±100	Decreasing with I_{exc}
Plasma temperature T_p for $T_l=5$ K (K)	≈20	≈15	Slightly increasing with $\hbar\omega_{exc}$
Chemical potential μ	2.542 eV±1 meV	1.822 V±2 meV	Varying with I_{exc}
Plasma binding energy $E_{EHP}^b=E_{ex}-\mu$ (meV)	≈10	≈3	
Drift length l_D (μm)	4±2	13±7	Under inhomogeneous excitation
Drift velocity v_D (cm/sec)	$\lesssim2.5\times10^6$ cm/sec	$\lesssim3\times10^6$ cm/sec	
Quasi-Fermi-energy E_F^e (meV)	37.0	24	CdS: $n_p=3\times10^{18}$ cm^{-3} $T_p=20$ K
Quasi-Fermi-energy E_F^h (meV)	6.8	7.5	CdSe: $n_p=8\times10^{17}$ cm^{-3} $T_p=15$ K
"Drift energy" (meV)			
$E_D^e=(m_e/2)v_D^2$	0.33	0.15	For $v_D=2\times10^6$ cm/sec
$E_D^h=(m_h/2)v_D^2$	1.8	0.67	

[a] From Refs. 28 and 43.

suming $v_D=2\times10^7$ cm/sec and $l_D=100$ μm) would lead to internal contradictions in the set of Eqs. (5)—(8). In particular, it should be noted that the value of n_p necessary to fit the observed spectral width of the gain spectra with the data given just above had to be $n_p \gg 2\times10^{18}$ cm^{-3}, while Eq. (7) would result in $n_p \ll 2\times10^{18}$ cm^3.

For CdSe one finds, from the experimental data in Fig. 15, a value for the lateral drift length of $l_D\approx20$ μm. The sublinear increase of the gain spectra with the sample thickness in Fig. 14 indicates, in a plot similar to that of Fig. 6(a), that one has already reached, for $5\lesssim d\lesssim10$ μm, the region where the initially linear increase of $\ln(I_T^*/I_T)$ bends over towards saturation. It seems therefore reasonable to assume for CdSe a longitudinal drift length of the order of 10 μm, in reasonable agreement with that for lateral drift.

Recent time-resolved psec luminescence experiments in CdSe (Ref. 3) also allow deduction of a value of l_D. The authors of Ref. 3 calculate a value $n_p^{calc}=5\times10^{19}$ cm^{-3} under the assumption that the electron-hole pairs stay in the volume given by the diameter of the excitation spot, $a=10$ μm, and the inverse absorption coefficient for the exciting light, $\alpha^{-1}(\hbar\omega_{exc})$, equal to 0.3 μm. From analysis of the luminescence spectra they deduce $n_p^{expt}\approx4\times10^{17}$ cm^{-3}, in reasonable agreement with our data. Assuming that the discrepancy between n_p^{calc} and n_p^{expt} is due to an expansion of the EHP into a hemisphere of radius l_D ($l_D\gtrsim a/2$), one obtains, for l_D,

$$l_D=\left[\frac{3}{8}\frac{n_p^{calc}}{n_p^{expt}}\frac{a^2}{\alpha(\hbar\omega_{exc})}\right]^{1/3}\approx7\ \mu\text{m}\ . \tag{9}$$

Evidently, the diffusion length of the plasma in CdSe is definitely larger than in CdS. There are two reasons to explain this. First, the lifetime of the EHP in CdSe is larger than in CdS. Values around 350 psec are given in the literature[3,41] (also see Table I). Second, all values of n_p measured so far in CdS are below the calculated equilibrium density n_0. This means that there is a trend in the plasma to condense into droplets. In CdSe one has $n_p\gtrsim n_0$. Consequently, the EHP tends to expand. Finally, it should be noted that the set of plasma parameters given for CdSe in Table I fulfills the conditions imposed by Eqs. (5)—(8).

The kinetic energies associated with the drift velocities are considerably smaller than the Fermi energies (Table I). The influence of v_D on the line shape of plasma gain and luminescence is thus of minor importance. On the other hand, v_D exceeds the value of the transverse velocity of sound v_{TA} by almost an order of magnitude. Thus, v_{TA} is not a strict upper limit for v_D for the materials and excitations conditions investigated here. A similar phenomenon has been found for GaAs, where the drift velocity v_h of the heavier carriers (the holes) has been investigated in an electric field **E** both experimentally and theoretically.[42] One finds that v_h increases with **E** up to values of $v_h=8\times10^6$ cm/sec and then saturates. Again,

one has $v_h^h \gg v_{TA}$. The value of 8×10^6 cm/sec is reached for $|\mathbf{E}| \approx 10^5$ V/cm.

Although the material parameters of GaAs are different from those of CdS or CdSe, some semiquantitative numbers may be deduced for our problem from Ref. 42. There the driving force is a gradient of the electrical potential ϕ. In the drift of the EHP the driving force could be a gradient of the chemical potential μ. An upper limit is $|\text{grad}\mu| \approx 0.5\times10^3$ V/cm in our experiments, assuming that μ tends to zero about 50 μm outside the excitation spot. According to Ref. 42, one would find, for GaAs, for $|\text{grad}\phi| = |\mathbf{E}| = 0.5\times10^3$ V/cm, a value $v_h \approx 0.8\times10^6$ cm/sec, in reasonable agreement with the data of Table I.

To summarize this part of the discussion, we found that one has a "slow drift" of the EHP both in CdS and CdSe. Up until now there has been no obvious reason to assume that the behavior of the EHP in other direct-band-gap materials like GaAs or CdTe should be completely different under comparable excitation conditions.

On the other hand, neither we nor—to our knowledge—anyone else is presently able to explain these values of v_D and l_D quantitatively. They are too large to be compatible with simple diffusion since a value of the diffusion coefficient D around 10^3 cm^2/sec would follow from $l_D = (D\tau_p)^{1/2}$. It is also not clear why Cherenkov-type emission of acoustic phonons does not limit the values of v_D to the velocity of sound in polar materials.

One point, which leads some authors to the assumption of fast drift, is spatially resolved luminescence experiments. As mentioned already in Ref. 11, these experiments must be considered with some care. As is well known, the high gain values connected with an EHP in direct-band-gap semiconductors generally give rise to superradiant emission mainly parallel to the excited surface of the sample, even if a resonator geometry of the crystal is avoided. This emission will leave the sample, e.g., at its edges, but it may also be scattered out of the sample by surface irregularities or scattering centers in the sample. Thus, experiments of spatially resolved luminescence probe not only the spatial distribution of the EHP, but also that of the emitted light and scattering centers. On the other hand, spatially resolved measurements of the EHP gain and the disappearance of the excitonic reflection are only sensitive to the EHP itself.

The other argument—for a "fast drift"—comes from a fit to the gain spectra with drift and **k** conservation alone. As discussed in Sec. IV, this fit overestimates both v_D and n_p. To demonstrate this, we show in Fig. 22 an observed gain spectrum of the EHP in CdTe from Ref. 19, together with two calculated ones. The material parameters used in the fit are given in Ref. 19. For the dashed curve only **k** conservation and drift are used. The values deduced from the fit are the same as in Ref. 19, namely $n_p = 6\times10^{17}$ cm^{-3}, $T_p = 16$ K, and $v_p = 1.2\times10^7$ cm/sec, indicating "fast drift." The dotted line has been calculated including **k** conservation, excitonic enhancement, and damping, but completely neglecting v_D, resulting in $n_p \approx 10^{17}$ cm^{-3} and $T_p \approx 8$ K.

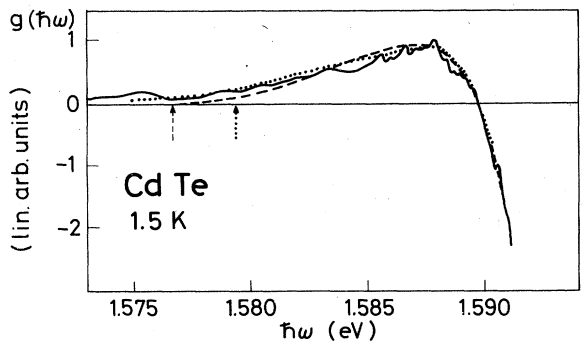

FIG. 22. Experimental plasma gain spectrum of CdTe from Ref. 19 fitted with the model involving only **k** conservation and drift (dashed line), and with a model without drift using **k** conservation damping and excitonic enhancement (dotted line). The positions of the reduced gap are indicated in both cases.

According to the above discussion this approximation may be made up to $v_D \approx 10^6$ cm/sec. The fit to the experimental curve is equally good. The value of the reduced gap lies for $n_p = 10^{17}$ cm^{-3}, only slightly below the lower calculated curve in Ref. 19, showing $E_g'(n_p)$, and thus again gives some support to the calculation of $E_g'(n_p)$ using the single-plasmon-pole approximation including plasmon-phonon mixed modes.

ACKNOWLEDGMENTS

The authors want to thank the Kristall- und Materiallabor der Universität Karlsruhe for the high-quality CdS and CdSe platelets, as well as Professor M. S. Razbirin for some very good CdSe crystals. Fruitful discussions are acknowledged with Professor Dr. H. Haug and Dr. S. Schmitt-Rink (Universität Frankfurt). It is a great pleasure to thank also Dr. A. Forchel, Dr. H. Schweizer, and Dr. H. Saito for partly controversial, but in all cases, stimulating discussions. This work was carried out under the auspices of the Sonderforschungsbereich "Festkörperspektroskopie" and was financed by the Deutsche Forschungsgemeinschaft.

[1]V. G. Lysenko, V. I. Revenko, T. G. Tartas, and V. B. Timofeev, Zh. Eksp. Teor. Fiz. **68**, 335 (1975) [Sov. Phys.—JETP **41**, 163 (1975)].

[2]M. Capizzi, S. Modesti, A. Frova, J. L. Staehli, M. Guzzi, and R. A. Logan, Phys. Rev. B **29**, 2028 (1984).

[3]Daly and H. Mahr, Phys. Rev. B **29**, 5591 (1984).

[4]G. O. Müller, H. H. Weber, and I. Höricke, Phys. Status Solidi B **91**, 531 (1979).

[5]K. Bohnert, G. Schmieder, and C. Klingshirn, Phys. Status Solidi B **98**, 175 (1980).

[6]O. Hildebrand, E. Göbel, K. M. Romanek, H. Weber, and G. Mahler, Phys. Rev. B **17**, 4775 (1978).

[7]K. Bohnert, M. Anselment, G. Kobbe, C. Klingshirn, H. Haug, S. W. Koch, S. Schmitt-Rink, and F. F. Abraham, Z. Phys. B **42**, 1 (1981).

[8]K. Bohnert, F. Fidorra, and C. Klingshirn, Z. Phys. B **57**, 263 (1984).

[9]Proceedings of the 3rd ICTP-IUPAP Semiconductor Symposi-

um on High Excitation and Short Pulse Phenomena, Trieste (1984) [J. Lumin. **30** (1985)].

[10]H. Saito, in Ref. 9, p. 303; Y. Unuma, Y. Abe, Y. Masumoto, and S. Shionoya, Phys. Status Solidi B **125**, 735 (1984).

[11]S. Modesti, A. Frova, J. L. Staehli, M. Guzzi, and M. Capizzi, Phys. Status Solidi B **108**, 281 (1981).

[12]K. Kempf and C. Klingshirn, Solid State Commun. **49**, 23 (1984).

[13]M. Capizzi, A. Frova, S. Modesti, A. Selloni, J. L. Staehli, and M. Guzzi, Helv. Phys. Acta (to be published).

[14]K. Kempf, Ph.D. thesis, Universität Frankfurt, 1984.

[15]F. A. Majumder, diplomathesis, Universität Frankfurt, 1984; H.-E. Swoboda, diplomathesis, Universität Frankfurt, 1985.

[16]D. Hulin, A. Antonetti, L. L. Chase, J. L. Martin, A. Migus, and A. Mysyrowicz, Opt. Commun. **42**, 260 (1982).

[17]T. M. Rice, in *Solid State Physics,* edited by H. Ehrenreich, F. Seitz, and D. Turnbull (Academic, New York, 1977), Vol. 32, p. 1; J. C. Hensel, T. G. Philips, and G. A. Thomas, *ibid.*, p. 88.

[18]R. Schwabe, F. Thuselt, H. Weinert, R. Bindemann, and K. Unger, Phys. Status Solidi B **89**, 561 (1978); D. Bimberg, M. S. Skolnick, and L. M. Sander, Phys. Rev. B **19**, 2231 (1979).

[19]H. Schweizer and E. Zielinski, in Ref. 9, p. 37; E. Zielinski, diplomathesis, Universität Stuttgart, 1983; H. Schweizer, Ph.D. thesis, Universität Stuttgart, 1984.

[20]S. W. Koch, *Dynamics of First Order Phase Transitions in Equilibrium and Nonequilibrium Systems,* Vol. 207 of *Lecture Notes in Physics,* edited by H. Ataki, J. Ehlers, K. Hepp, R. Kippenhahn, H. A. Weidenmüller, and J. Zittartz (Springer, New York, 1984).

[21]O. Hildebrand, F. Faltermaier, and M. H. Pilkuhn, Solid State Commun. **19**, 841 (1976).

[22]M. Rösler and R. Zimmermann, Phys. Status Solidi B **67**, 525 (1975); R. Zimmermann, *ibid.* **86**, K63 (1978).

[23]H. Haug and D. B. Tran Thoai, Phys. Status Solidi B **98**, 581 (1980).

[24]C. Klingshirn and H. Haug, Phys. Rep. **70**, 315 (1981).

[25]H. Haug, Adv. Solid State Phys. **22**, 149 (1982); H. Haug and S. Schmitt-Rink, Prog. Quant. Electron. **9**, 3 (1984).

[26]A. Forchel, H. Schweizer, and G. Mahler, Phys. Rev. Lett. **51**, 501 (1983).

[27]G. Mahler, in Ref. 9, p. 18.

[28]*Landolt-Börnstein,* New Series, Group III, Vol. 17b, edited by O. Madelung, M. Schulz, and H. Weiss (Springer, Berlin, Heidelberg, New York, 1982).

[29]K. M. Romanek, H. Nather, J. Fischer, and E. O. Göbel, J. Lumin. **24-25**, 585 (1981).

[30]A. Cornet, M. Pugnet, J. Collet, T. Amand, and M. Broussaeu, J. Phys. (Paris) Colloq. **42**, C7-47 (1981).

[31]A. Cornet, T. Amand, M. Pugnet, and M. Brousseau, Solid State Commun. **43**, 147 (1982).

[32]J. P. Wolfe, Ref. 9, p. 82.

[33]A. Forchel, B. Laurich, H. Hillmer, G. Trankle, and M. Pilkuhn, Ref. 9, p. 67.

[34]A. Kreissl, K. Bohnert, V. G. Lyssenko, and C. Klingshirn, Phys. Status Solidi B **114**, 537 (1982).

[35]V. G. Lyssenko and V. I. Revenko, Fiz. Tverd. Tela (Leningrad) **20**, 2144 (1978) [Sov. Phys.—Solid State **20**, 1238 (1978)].

[36]M. Rösler and R. Zimmermann, Phys. Status Solidi B **83**, 85 (1977); R. Zimmermann, K. Kilimann, W. D. Kraeft, D. Kremp, and R. Röpke, *ibid.* **90**, 175 (1978).

[37]G. Beni and T. M. Rice, Phys. Rev. B **18**, 768 (1978); Phys. Rev. Lett. **37**, 874 (1976).

[38]H. Kalt, V. G. Lyssenko, R. Renner, and C. Klingshirn, Solid State Commun. **51**, 675 (1984).

[39]C. Klingshirn, K. Bohnert, H. Kalt, V. G. Lyssenko, and K. Kempf, in Ref. 9, p. 188.

[40]H. Yoshida, H. Saito, S. Shionoya, and V. B. Timofeev, Solid State Commun. **33**, 161 (1980); H. Yoshida, H. Saito, and S. Shionoya, J. Phys. Soc. Jpn. **50**, 881 (1981).

[41]M. Yoshida, H. Saito, and S. Shionoya, Phys. Status Solidi B **104**, 331 (1981).

[42]K. Brennan and K. Hess, Phys. Rev. B **29**, 5581 (1984).

[43]G. Blattner, G. Kurtze, G. Schmieder, and C. Klingshirn, Phys. Rev. B **25**, 7413 (1982).